Biochimica et Biophysica Acta 1798 (2010) 947–957

Contents lists available at ScienceDirect

Biochimica et Biophysica Acta

journal homepage: www.elsevier.com/locate/bbamem

Effects of protons on macroscopic and single-channel currents mediated by the human P2X7 receptor

B. Flittiger [a], M. Klapperstück [a], G. Schmalzing [b], F. Markwardt [a,*]

[a] Julius-Bernstein-Institute for Physiology, Martin-Luther-University Halle, Magdeburger Straße 6, D-06097 Halle/Saale, Germany
[b] Molecular Pharmacology, RWTH Aachen University, Wendlingweg 2, D-52074 Aachen, Germany

ARTICLE INFO

Article history:
Received 6 October 2009
Received in revised form 18 January 2010
Accepted 28 January 2010
Available online 4 February 2010

Keywords:
P2 purinergic receptor
P2X7 receptor
pH dependence
Patch clamp

ABSTRACT

Human P2X7 receptors (hP2X7Rs) belong to the P2X family, which opens an intrinsic cation channel when challenged by extracellular ATP. hP2X7Rs are expressed in cells of the inflammatory and immune system. During inflammation, ATP and protons are secreted into the interstitial fluid. Therefore, we investigated the effect of protons on the activation of hP2X7Rs. hP2X7Rs were expressed in *Xenopus laevis* oocytes and activated by the agonists ATP or benzoyl-benzoyl-ATP (BzATP) at different pH values. The protons reduced the hP2X7R-dependent cation current amplitude and slowed the current deactivation depending on the type and concentration of the agonist used. These effects can be explained by (i) the protonation of ATP, which reduces the effective concentration of the agonist ATP^{4-} at the high- and low-affinity ATP activation site of the hP2XR, and (ii) direct allosteric inhibition of the hP2X7R channel opening that follows ATP^{4-} binding to the low-affinity activation site. Due to the hampered activation via the low-affinity activation site, a low pH (as observed in inflamed tissues) leads to a relative increase in the contribution of the high-affinity activation site for hP2X7R channel opening.

1. Introduction

P2X7 receptors (P2X7Rs) belong to the P2X family of ligand-gated channels that are opened by extracellular ATP. The expression of P2X7Rs in leukocytes infers a function within the immune and inflammatory system. Consistent with this view, activation of P2X7Rs induces the release of the inflammatory mediator interleukin 1β from macrophages [1–3]. In macrophages, P2X7Rs play a role in actin assembly, which is important for phagocytosis and the fusion of phagosomes with lysosomes [4,5]. Furthermore, P2X7Rs are involved in nociception [6–8] and have been pursued as a promising drug target for the treatment of inflammatory and chronic pain [9–12].

Inflammation is usually accompanied by acidosis [13–15], and several nociceptors are activated by extracellular protons [16–18]. A study of the effect of protons on P2X7Rs is therefore of interest as it may help in the understanding of their function in inflamed tissue. The numerous possible effects of protons complicate the delineation of the underlying mechanisms. In principle, protons may influence the ion channel pore conduction, the receptor binding of the agonist or the agonist-induced pore opening (gating). Additionally, the binding of protons to ATP^{4-} reduces the concentration of the P2X7R agonist, free ATP^{4-}. Following activation of the P2X7R, any experimental measurement (such as the fluorescence signals reflecting intracellular calcium concentration or the uptake of fluorescence dye) may be altered by the pH. Even if an early signal of P2X7R activation, the induction of a cell membrane current, is measured, secondary activation of additional ion current conductances [19–22] may lead to misinterpretations of the effect of protons on the P2X7R.

Here, we designed experiments to minimize the contaminating side effects of pH changes on hP2XR-dependent currents. Measurements in the oocyte expression system allowed us to record hP2X7R-dependent currents in divalent cation-free extracellular solutions. Thus, the complexing effects of Ca^{2+} or Mg^{2+} at ATP and the possible allosteric effects of these cations on the hP2X7R were excluded. Additionally, the effect of P2X7R-dependent pore formation [23] is obviously absent if hP2XRs are expressed in *Xenopus* oocytes [24]. To unequivocally determine the influence of pH on authentic hP2X7R-mediated currents that are free of contaminating secondarily activated ion fluxes, we also determined the effects of protons on hP2X7R-dependent single-channel events [25]. As we have previously shown, activation of hP2X7R is mediated via high and low-affinity activation sites [26,27]. Here we report that protons differently affect hP2X7R dependent current induction via these two activation site types.

2. Materials and methods

2.1. Ethical approval

Xenopus laevis females were imported from *Xenopus* Express (Vernassal, France). Altogether, about 20 animals were anaesthetized

Abbreviations: ATP^{4-}, free form of ATP, not bound to cations; BzATP, 2′3′-O-(4-benzoyl)-benzoyl-ATP; hP2X7R, human purinergic P2X7 receptor; V_h, holding potential

* Corresponding author. Tel.: +49 345 557 1390/1396; fax: +49 345 55 27899.
E-mail address: fritz.markwardt@medizin.uni-halle.de (F. Markwardt).

0005-2736/$ – see front matter © 2010 Elsevier B.V. All rights reserved.
doi:10.1016/j.bbamem.2010.01.023

in an aqueous solution supplemented with 0.2% tricaine (ethyl 3-aminobenzoate methanesulfonate, Sigma, Deisenhofen, Germany) for 20 min and thereafter placed on a wet platform for laparotomy. Parts of the ovary were removed through a small incision which was thereafter closed by sutures of the peritoneum and the outer skin. Frogs awake after the operation within about 20 min in a box half filled with water to leave the head free for breathing. The frog was allowed to recover for at least two months before removal of another batch of oocytes. Keeping of and operation on frogs were approved by the local animal welfare committee (ref no. 53a-42502/2-173) and are in compliance with The Journal of Physiology's guidelines for experimentation on animals [28].

2.2. Chemicals

Chemicals were obtained from Sigma if not otherwise stated. Na_2ATP was purchased from Roche (Mannheim, Germany).

2.3. The expression of the hP2X7R in X. laevis oocytes

A plasmid encoding the human P2X7 subunit (hP2X7, accession no. Y09561, [29] was available from previous studies [24]. The $S^{339}Y$-hP2X7 mutant was generated using the QuickChange site-directed mutagenesis kit (Stratagene, Heidelberg, Germany) and verified by commercial sequencing (MWG, Ebersberg, Germany). Capped, poly-adenylated cRNAs were synthesized, purified and injected at 0.01–0.5 μg/μl (~23 nl/oocyte) into collagenase-defolliculated oocytes as described previously [24]. Until their use one to three days later, the oocytes were kept at 19 °C in oocyte Ringer solution (ORi) consisting of 100 mM NaCl, 1 mM KCl, 1 mM $CaCl_2$, 1 mM $MgCl_2$ and 5 mM Hepes supplemented (per ml) with 100 U penicillin and 100 μg streptomycin.

2.4. Two-electrode voltage-clamp electrophysiology

Two-electrode voltage-clamp recordings were performed on healthy stage V–VI oocytes at room temperature (≈22 °C) essentially as described previously [24]. Microelectrodes were filled with 3 M KCl (the resistances were 0.9–1.3 MΩ). The currents were recorded and filtered at 100 Hz using an oocyte clamp amplifier (OC-725C, Hamden, USA) and sampled at 85 Hz. The impalement of the electrodes and the measurement of the membrane potential of the oocytes were carried out in ORi solution (see above). For subsequent recordings of the P2X7R-dependent currents, the oocytes were superfused with a nominally Ca^{2+}- and Mg^{2+}-free solution containing (in mM) 100 NaCl, 2.5 KCl, 5 Hepes, 0.1 EGTA and 0.1 flufenamic acid, at pH 7.4 and a holding potential (V_h) of −40 mV. Ca^{2+} and Mg^{2+} were omitted to avoid the activation of endogenous currents by Ca^{2+} influx through the P2X7R channels and to prevent the complexation of ATP^{4-}. The inclusion of flufenamic acid prevented the development of a large conductance that is otherwise seen in divalent cation-free solutions. We achieved a fast and reproducible exchange between the different bathing solutions within <1 s using a small chamber (0.1 ml) combined with fast superfusion (75 μl/s) and a set of computer-controlled magnetic valves [30]. We invoked hP2X7R-dependent inward currents by switching for 6 s to a bathing solution that contained additional ATP or 2′3′-O-(4-benzoyl)-benzoyl-ATP (BzATP) at the concentrations and pH values indicated in the text and figures. We measured the pH values of all solutions at the end of the experiments, and they were unchanged.

Taking the pH-dependent protonation of ATP^{4-} into account, the free ATP^{4-} and $BzATP^{4-}$ concentrations were calculated according to:

$$\left[agonist^{4-}\right] = \frac{[agonist]}{1 + 10^{pK-pH}}. \quad (1)$$

In these calculations, we used a pK value for the protonation of ATP^{4-} of 6.51 [31]. For BzATP, the same pK value was used.

Patch pipettes were pulled from borosilicate glass, coated with Sylgard (Dow Corning Corp., Midland, MI, USA) and filled with a solution consisting of (in mM): 90 aspartic acid, 10 CsCl, 10 EGTA, 10 BAPTA, 10 Hepes and 0.5 $MgCl_2$. The pH was adjusted to 7.2 using CsOH. The patch pipettes had resistances between 5 and 15 MΩ as measured in the patch bathing solution. We recorded the currents using an Axopatch 1D patch clamp amplifier (Axon Instruments, Foster City, CA, USA). hP2X7R-dependent currents were filtered at 1 kHz and sampled at 5 kHz, S339Y-hP2X7R-dependent currents were filtered at 5 kHz and sampled at 20 kHz.

Single-channel recordings were performed in the outside-out configuration of the patch clamp technique as described recently [25]. We achieved a fast and reproducible exchange of the different solutions at the extracellular site of the patch using a combination of a U-tube technique [30] and a piezo-driven liquid filament switch [32]. The pipette with the membrane patch was perfused with the patch bathing solution containing (in mM): 100 NaCl, 0.5 $CaCl_2$ and 5 Hepes, at pH 7.4. The ATP^{4-} concentrations and the pH values of the liquid filament solutions that flowed out of the U-tube (the U-tube solution) are given in the figures and in the text.

The current data were stored and analyzed on a personal computer using software programmed at our department (Superpatch 2000, SP-Analyzer by T. Böhm) and the computer program ASCD (generously provided by G. Droogmans, Catholic University Leuven, Belgium). The averaged data are reported as the mean ± SD; N is the number of experiments. We made nonlinear approximations and presented the data using the program Sigmaplot (SPSS). The resulting parameters were expressed as the mean ± SEM. The statistical data were analyzed using one-way ANOVA ($P<0.05$). The statistical significance of the differences between the means was tested using the multiple t-test (Bonferroni) included in the program Sigmastat (SPSS, Chicago, USA).

3. Results

3.1. The extracellular effects of pH on the hP2X7R-dependent whole cell currents

hP2X7R-dependent whole cell currents were recorded from *X. laevis* oocytes in the two-electrode voltage-clamp configuration. As divalent cation-free bathing solutions were used and defolliculated oocytes lack ectonucleotidase [33] protons were the only relevant extracellular constituents that were able to change the ATP^{4-} concentration. Fig. 1 shows typical whole cell current traces that were elicited by ATP (Fig. 1A) or BzATP (Fig. 1B) in hP2X7R-expressing oocytes at different pH values. Acidification from pH 7.4 to 6.4 markedly decreased the ATP-induced current amplitude and slowed the deactivation time course. In contrast, a decrease in the acidity from pH 7.4 to 8.4 produced only a slight (for ATP) to moderate (for BzATP) increase in the current amplitude.

The deactivating current $I_{deact}(t)$ during the washout of ATP can be quantitatively described by a bi-exponentially decaying function:

$$I_{deact}(t) = I_{deact,fast} \cdot e^{-\frac{t}{\tau_{deact,fast}}} + I_{deact,slow} \cdot e^{-\frac{t}{\tau,deact,slow}} + I_0 \quad (2)$$

where I_0 is the steady-state current without ATP, $I_{deact,fast}$ and $I_{deact,slow}$ are the initial amplitudes, and $\tau_{deact,fast}$ and $\tau_{deact,slow}$ are the time constants of the fast and slowly deactivating current component, respectively [26,27]. Fitting the data to Eq. (2) revealed that the time constants for the fast and slow deactivation were not significantly influenced by the pH (data not shown). For both agonists, ATP and BzATP, the slower overall deactivation time course at pH 6.4, as compared to pH 7.4, can be attributed simply to a reduction in the contribution of the fast-deactivating current component to the total

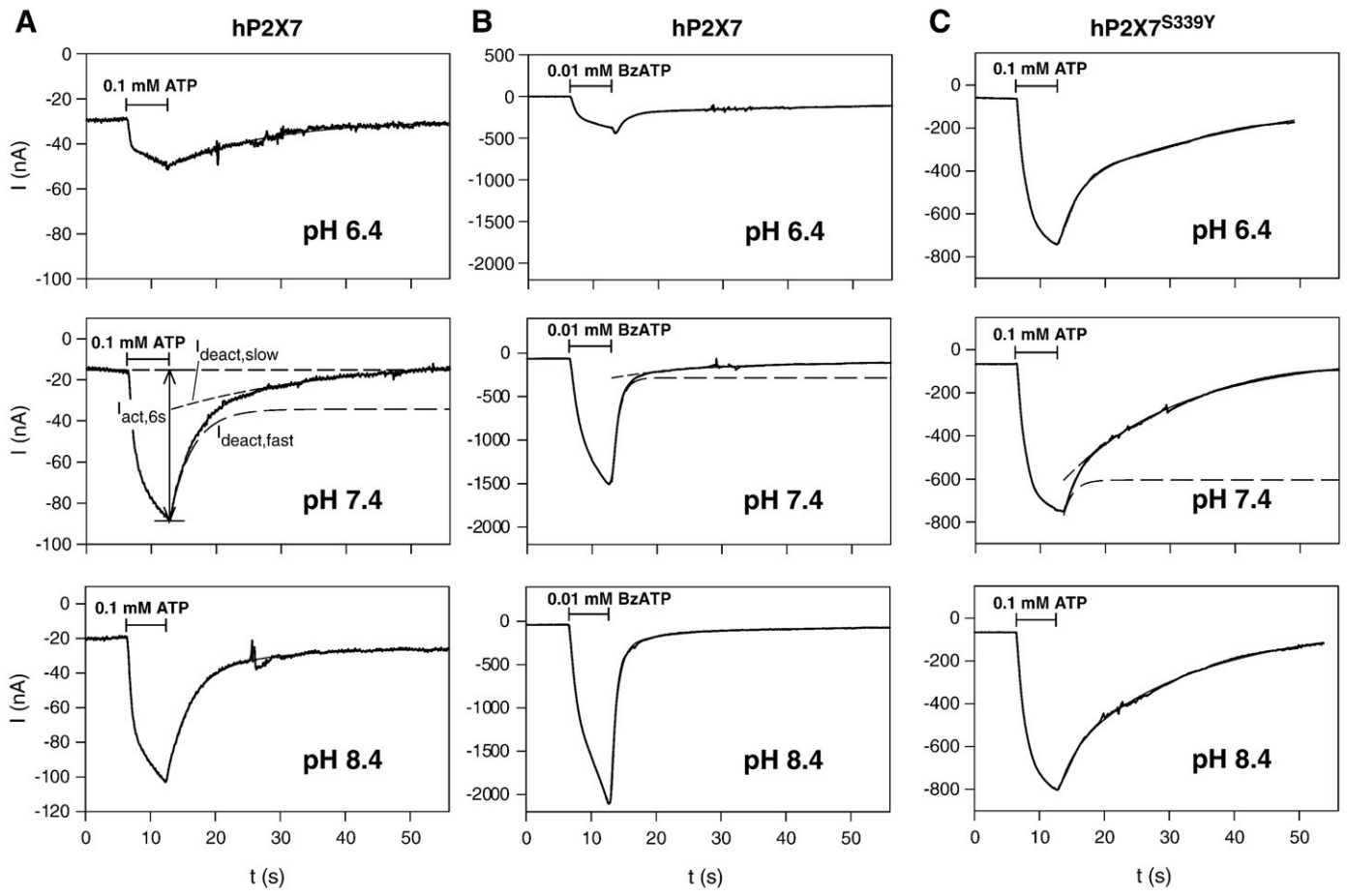

Fig. 1. The effect of the pH of the media on the hP2X7R-dependent inward currents recorded from intact *X. laevis* oocytes. Representative current traces are shown that were elicited by ATP or BzATP as indicated from oocytes expressing the wt-hP2X7R (A, B) or the S^{339}Y-hP2X7R mutant (C). The timing of agonist application and the pH of the agonist-containing media are also indicated. The middle panel of (A) illustrates an example of the hP2X7R-dependent total current amplitude $I_{act,6s}$. All middle panels show the two components of the deactivating current that are characterized by the fast ($I_{deact,fast}$) and slow ($I_{deact,slow}$) exponential decay rates as approximated by Eq. (2). The approximated deactivation time courses are depicted as superimposed smooth short and long dashed curves. The currents that were measured using the three pH values of the media in A, B or C were recorded using the same oocyte. The fast, transient current changes are artifacts that arose during washout.

current decline (Fig. 2A, B). As the fast-deactivating current component corresponds to the current that is activated by the low-affinity ATP activation site [26,27], the main influence of the extracellular protons seems to be directed toward the low-affinity activation site.

To investigate the effect of protons on the high- and low-affinity agonist activation sites of the hP2X7Rs in greater detail, we determined the agonist concentration–response curves at three different pH values (Fig. 3). The concentration–response curves of the relative activating currents I_{rel} were fitted by:

$$I_{rel}([agonist]) = \frac{I_{act,6s}(\mathrm{pH}, [agonist])}{I_{act,6s}(7.4, [0.1\,\mathrm{mM\,ATP}])} = \frac{I_{rel,\infty,1}}{\left(1 + \frac{10^{pK_{D,1}}}{[agonist]}\right)^2} + \frac{I_{rel,\infty,2}}{\left(1 + \frac{10^{pK_{D,2}}}{[agonist]}\right)^2} \quad (3)$$

where $I_{act,6s}$ was measured as shown in Fig. 1 and normalized to the current induced by 0.1 mM ATP at pH 7.4, and $pK_{D,1}$ and $pK_{D,2}$ are the negative decadic logarithms of the apparent ATP dissociation constants of the putative high- and low-affinity activation sites [26,27], respectively. $I_{rel,\infty,1}$ and $I_{rel,\infty,2}$ are the maximal amplitudes at agonist concentrations that saturated the high- and low-affinity activation sites, respectively. For all of the data, Hill coefficients of 2 for both sites resulted in higher correlation coefficients than did Hill coefficients of 1 or >2. All of the concentration–response curves for wt-hP2X7R activation were significantly better described by this model of two different independent activation sites than by a model with only one type of activation site [34].

BzATP, the most potent P2X7R agonist, predominantly activates the low-affinity activation site of the wt-hP2X7R, and has not only a higher potency (i.e., a lower K_D), but also a much higher efficacy (a higher I_{max} at saturating agonist concentrations) than ATP at this site (Fig. 3 and [24]. In addition, at the high-affinity activation site, BzATP possesses a higher potency than ATP, but the efficacies of BzATP and ATP are equal at this site (Fig. 3 and Table 1).

Acidification of the media from pH 7.4 to 6.4 mainly reduced the amplitude of the current component that is evoked by activation of the low-affinity activation site and the pK_D values for the high- and low-affinity activation sites (Table 1). To examine whether the lower apparent K_D values at low pH values resulted from a decrease in the free agonist^{4-} concentration by protonation, we plotted the agonist^{4-} concentration–response curves (Fig. 3B). At low agonist concentrations (at which the high-affinity activation site was mainly activated), the curves obtained for the same agonist at different pH values overlapped and the calculated K_D values became pH-independent. This indicates that the effect of protons in the low agonist concentration range predominantly originate from pH-dependent changes in [agonist^{4-}]. This indirectly supports the view that the fourfold negatively charged agonist species represents the genuine hP2X7R agonist, rather than the protonated (and hence less negatively charged) agonist species.

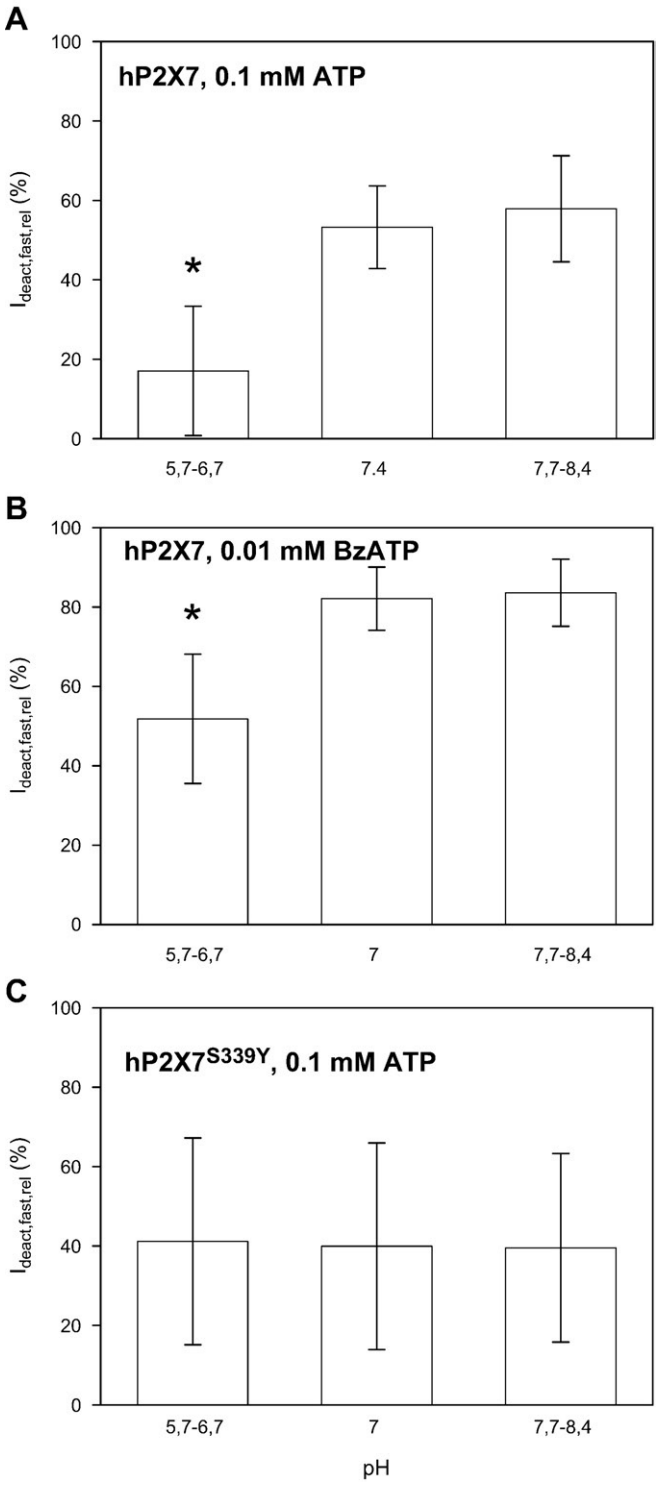

Fig. 2. The effect of the pH of the media on the deactivation time course of the hP2X7R-dependent currents. The oocyte-expressed hP2X7 constructs and agonists that were used are indicated. The currents were recorded and analyzed as described in the legend to Fig. 1. The contribution of the fast-deactivating current component was calculated according to $I_{deact,fast,rel} = I_{deact,fast} / (I_{deact,fast} + I_{deact,slow})$, with $N = 7–27$ oocytes. Statistically significant differences are marked by asterisks.

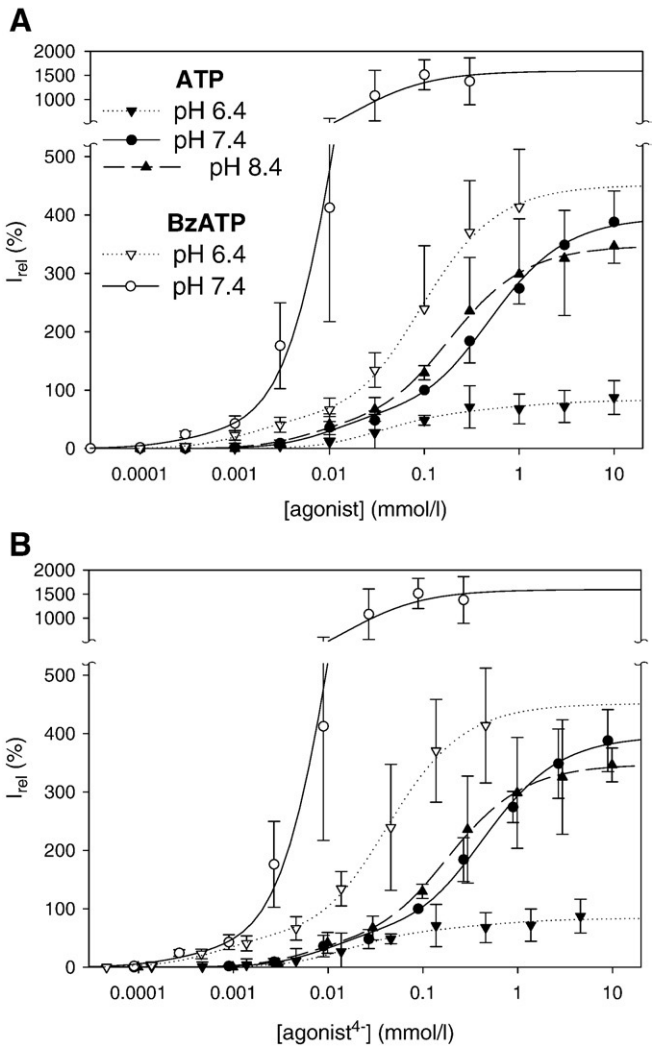

Fig. 3. The dependence of the agonist concentration–response behavior of the hP2X7Rs on the extracellular pH. The amplitudes of the agonist-induced currents were normalized, fitted by Eq. (3) and plotted against the total agonist concentration (A) and the free agonist concentration (B) (as calculated by Eq. (1)). The values listed are the means from 4 to 26 oocytes. The fitted results are listed in Table 1.

In addition, at higher agonist concentrations that also activate the low-affinity activation site, the reduction of the agonist potency in acidic media can be well explained by taking the reduction of the free agonist^{4-} concentration by protonation into account. However, independent of the free ATP^{4-}, the protons reduced the efficacy of ATP at the low-affinity activation site in terms of the maximal current that is activatable by the respective agonist (Fig. 3 and Table 1).

3.2. The extracellular effect of pH on the low-affinity activation-site-lacking $S^{339}Y$-hP2X7R mutant

To investigate the effect of protons on the high-affinity activation site we used the $S^{339}Y$-hP2X7R. The $S^{339}Y$-hP2X7R-dependent currents can be characterized using a monophasic ATP concentration–response curve with a single apparent K_D value of about 0.5 μM ATP, which is saturating in the micromolar concentration range (Fig. 4A). This strongly suggests that the $S^{339}Y$-hP2X7R mutant is activated exclusively through the high-affinity activation site. Furthermore, BzATP activates the $S^{339}Y$-hP2X7R mutants with a much higher potency than does ATP, whereas the efficacies of BzATP and ATP are equal (Fig. 4A). Acidification of the medium from pH 7.4 to 6.4 inhibited the ATP-induced $S^{339}Y$-hP2X7R currents (Fig. 4A), mostly by reducing the concentration of the genuine agonist ATP^{4-} through protonation (Fig. 4B, Table 1). The $S^{339}Y$-hP2X7R mutant deactivated slowly (Fig. 1C), as it is characteristic for the current component that is activated by the high-affinity activation site of the wt-hP2X7R [26,27]. Changing the extracellular pH did not alter the deactivation

Table 1
The influence of the pH of the media on the concentration–response behavior of ATP and BzATP at the wt-hP2X7R (wt) and the $S^{339}Y$-hP2X7R mutant ($S^{339}Y$).

	$I_{rel,\infty,1}$ (%)	$I_{rel,\infty,2}$ (%)	$pK_{D,1}$ (agonist)	$pK_{D,1}$ (agonist^{4-})	$pK_{D,2}$ (agonist)	$pK_{D,2}$ (agonist^{4-})
wt, ATP pH 6.4	70 ± 9	13 ± 9[a]	4.8 ± 0.1[a]	5.1 ± 0.1	3.2 ± 0.5	3.5 ± 0.5
wt, ATP pH 7.4	80 ± 15	317 ± 14	5.2 ± 0.2	5.2 ± 0.2	3.7 ± 0.3	3.7 ± 0.3
wt, ATP pH 8.4	64 ± 14	284 ± 13	5.4 ± 0.2	5.4 ± 0.2	4.0 ± 0.1	4.0 ± 0.1
wt, BzATP pH 6.4	67 ± 15	384 ± 15[a]	6.1 ± 0.2[a]	6.4 ± 0.3	4.4 ± 0.2[a]	4.7 ± 0.2
wt, BzATP pH 7.4	50 ± 23	1554 ± 163	6.7 ± 0.2	6.7 ± 0.2	5.1 ± 0.2	5.1 ± 0.2
$S^{339}Y$, ATP pH 6.4	105 ± 4	–	5.5 ± 0.1[a]	5.9 ± 0.1[a,b]	–	–
$S^{339}Y$, ATP pH 7.4	102 ± 2	–	6.2 ± 0.05	6.2 ± 0.05	–	–
$S^{339}Y$, BzATP pH 7.4	101 ± 2	–	6.9 ± 0.05[a]	6.9 ± 0.05[a]	–	–

The parameters were calculated using Eq. (3).
[a] Statistically significant differences from the approximated values at pH 7.4.
[b] The statistically significant difference between the approximated values for the total agonist concentration (agonist) and the free agonist concentration (agonist^{4-}).

time course (Fig. 2C). These findings support the view that extracellular protons mainly affect the low-affinity activation site of hP2X7Rs.

3.3. Proton concentration-dependent current amplitudes of the wt-hP2X7R and the $S^{339}Y$-hP2X7R mutant

Next, the effect of medium pH on the hP2X7R-mediated currents was investigated over a broader pH range (Fig. 5). Since the pH effect was influenced by the concentration of the agonist (Fig. 5A, B), the pH dependence of the agonist-induced hP2X7R-mediated currents was approximated by:

$$I_{rel}([pH]) = \frac{I_{act,6s}(pH, [agonist])}{I_{act,6s}(7.4, [0.1\,mM\,ATP\,or\,0.01\,mM\,BzATP])} = \frac{I_{rel,\infty}}{\left(1 + \frac{10^{-pH}}{10^{pK_H}}\right)^3} + c \quad (4)$$

where the ATP- and BzATP-induced currents were normalized to those evoked at pH 7.4 by 0.1 mM ATP or 0.01 mM BzATP, respectively. pK_H is the negative decadic logarithm of the apparent proton dissociation constant, and $I_{rel,\infty}$ and c are the extrapolated current amplitudes at zero and the infinite extracellular proton concentration, respectively. Hill coefficients of 3 gave the highest correlation coefficients in the computer fits.

Acidification exerted a stronger effect on the hP2X7R-mediated currents that were elicited by 10 µM BzATP than on those that were elicited by 1 µM BzATP. Both the high- and low-affinity activation sites of hP2X7R are activated when using 10 µM BzATP, but at this concentration, most of the current originates from the activation at the low-affinity activation site. At 1 µM BzATP, it is the high-affinity activation site that is primarily activated. The concentration-dependent effect of acidification can be explained by assuming that protons have two modes of action, one of which operates through the protonation of ATP^{4-}, which has a pK_D of 6.51 [31]. Protonation of ATP^{4-} diminishes [ATP^{4-}] as the active agonist form and, thus, the effective agonist concentration at both the high- and low-affinity activation sites. The second mode of proton action seems to stem from a direct effect on the hP2X7R itself and involves a reduction of the current originating from the activation of the low-affinity activation site. This proton effect is predominant if the hP2X7R is activated primarily through the low-affinity activation site, as is the case when using 10 µM BzATP. From the data in Fig. 5B, a pK_D value of about 6.8 can be inferred for the protonation of the hP2X7R (Table 2).

A similar agonist concentration-dependent pH effect was observed when ATP was used for hP2X7R activation (Fig. 5A). This suggests that protons affect the activation of the hP2X7R by ATP through the same mechanisms as outlined above for BzATP. Since protons exert distinct effects on the hP2X7R that depend on the concentration of the activating agonist, the computational modeling of the data by Eq. (4) must be regarded as an oversimplification. Therefore, it represents only a descriptive approximation.

As detailed above, the $S^{339}Y$-hP2X7R mutant can be conceived, in terms of electrophysiological function, as an hP2X7R that possesses

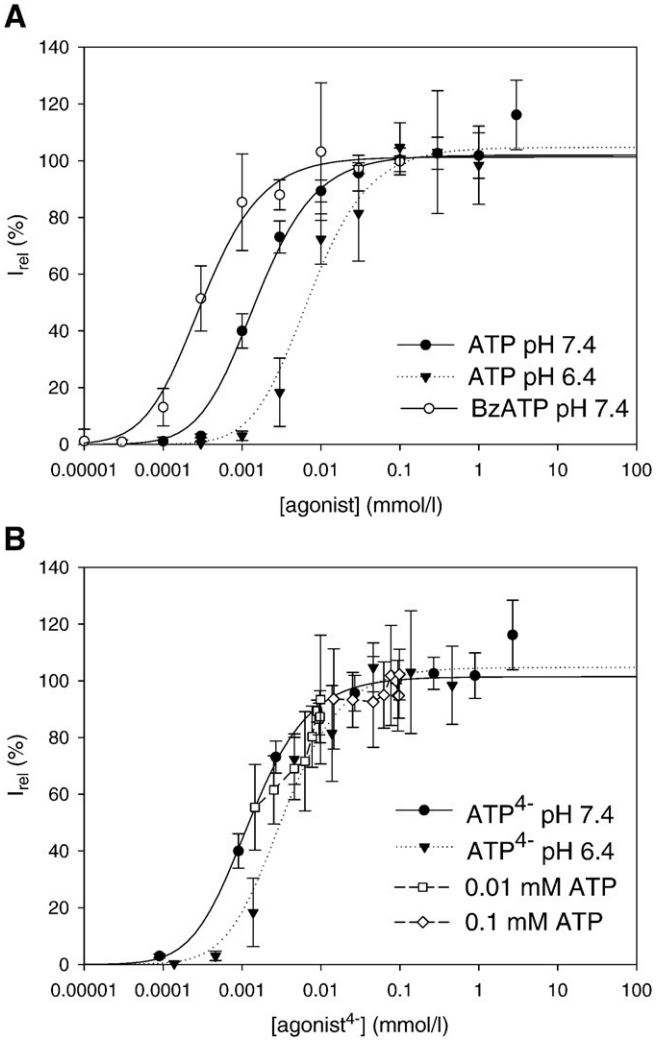

Fig. 4. The influence of the pH of the media and the agonist type on the concentration–response behavior of the $S^{339}Y$-hP2X7R mutant. The relative amplitudes of the agonist-induced currents were calculated, fitted according to Eq. (3) (with $I_{rel,\infty,2} = 0$) and plotted against total [agonist] (A) and [$agonist^{4-}$] (B). The open symbols in (B) represent the ATP^{4-} dependence of the current evoked by 0.01 or 0.1 mM ATP at different pH normalized to $I_{act,6s}$ at a pH of 7.4 from Fig. 5C. The corresponding ATP^{4-} concentrations were calculated using Eq. (1). The values are the means from 4 to 19 oocytes. The fitted results are listed in Table 1.

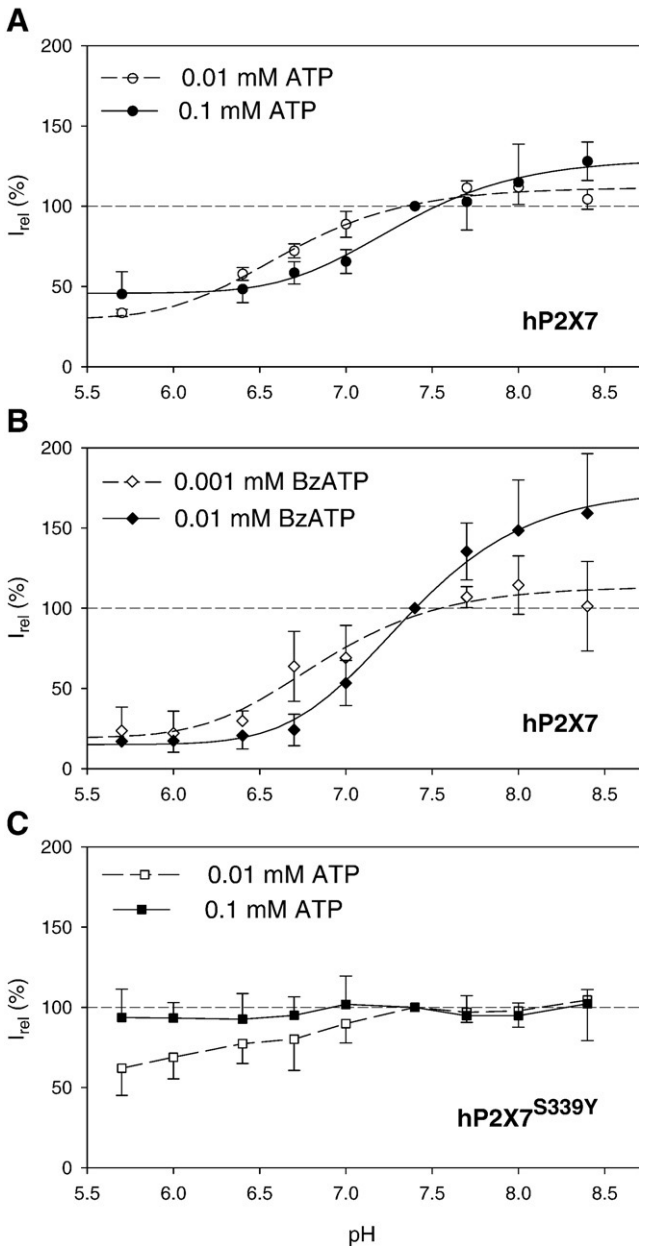

Fig. 5. The effect of the pH of the media on the activation of the hP2X7R. The currents were measured on oocytes that were expressing the wt-hP2X7 or the S^{339}Y-hP2X7R mutant after application of the agonists ATP or BzATP as indicated, following the protocol of Fig. 1. After normalization to the currents evoked at pH of 7.4, the current amplitudes were plotted against pH. The normalized currents that are shown in (A, B) were also fitted using Eq. (4). $N = 4$–20 oocytes. The fitted results are listed in Table 2.

only the high-affinity activation site. Variations in the pH between 5.7 and 8.4 at a comparably high total concentration of 100 μM ATP had only a negligible effect on the S^{339}Y-hP2X7R-mediated currents. This can be easily explained by the absence of the low-affinity activation site and, accordingly, by the lack of the direct inhibitory effect of acidification on the S^{339}Y-hP2X7R channel function. Also consistent with our expectations, the current mediated by activation of the high-affinity activation site did not respond to pH-dependent changes in free ATP^{4-} concentrations at 100 μM total ATP, because the lowest free concentration of 0.015 mM ATP^{4-} that is achieved at the lowest medium pH investigated (5.7) was still saturating at the high-affinity activation site. In the sub-saturating concentration range (0.01 mM ATP in Fig. 5B), however, an inhibiting effect of the protons on the S^{339}Y-hP2X7R-dependent currents became apparent. This effect can be fully attributed to protonation-dependent changes of ATP^{4-}, because the concentration–response curves that were obtained at pH 7.4 and 6.4 and those recalculated from the measured pH effect at 0.1 and 0.01 mM ATP (Fig. 5C) overlap when considered in terms of the concentration of free ATP^{4-} rather than total ATP (Fig. 4B).

Table 2
The effect of the extracellular protons on the activation of the wt-hP2X7R and the S^{339}Y-hP2X7R mutant.

	$I_{rel,\infty}$ (%)	c (%)	pK_H
0.01 ATP	82 ± 4	30 ± 4	6.1 ± 0.1
0.1 ATP	86 ± 5	46 ± 4[a]	6.7 ± 0.1[a]
0.001 BzATP	94 ± 7	19 ± 6	6.3 ± 0.1
0.01 BzATP	159 ± 4[a]	15 ± 3	6.8 ± 0.1[a]

The parameters were calculated using Eq. (4).
[a] Statistically significant differences from the parameters calculated for the respective lower agonist concentrations.

3.4. Extracellular pH effects on the wt-hP2X7R at the single-channel level

The pH dependence of the hP2X7R was also examined at the single-channel level using outside-out patches that were excised from hP2X7R-expressing *X. laevis* oocytes. Since resolvable hP2X7R-dependent single-channel events are fully dependent on the low-affinity activation sites [25,27], only pH effects on currents resulting from activation of this hP2X7R site are reported by single-channel measurements. Protons may (i) act within the channel pore, (ii) interfere with the binding of ATP^{4-} to the hP2X7R and/or (iii) allosterically affect the hP2X7R gating. To assess possibility (i), we investigated the pH effect on open channels. Variations in the pH between 6.4 and 8.4 did not affect the single-channel current conductance, the reversal potential (Fig. 6) or the single-channel current amplitude (Fig. 7A–G). The open probability, however, decreased with pH (Fig. 7D–F, H). Single-channel current analysis revealed this to be due to a longer duration in the closed state (Fig. 8D–F, H). The mean open time, on the other hand, was not affected by pH (Fig. 8A–C, G).

To assess possibilities (ii) and (iii), the effect of acidic pH on the agonist concentration-dependence of single hP2X7R channels was investigated by measuring the ATP concentration–response curve of the average ensemble current of multi-channel patches (Fig. 9). The currents were normalized to the mean current evoked by 5.8 mM ATP at pH 7.4. The concentration–response curves at pH 6.4 and 7.4 were fitted by Eq. (3), assuming only that the low-affinity activation site is the relevant one for channel opening (i.e., $I_{rel,\infty,2} = 0$). The effect of lowering the pH from 7.4 to 6.4 can be explained by the protonation of ATP^{4-} (as reflected by the increased K_D) and an additional reduction of the efficacy of ATP^{4-} (as reflected by the reduced $I_{rel,\infty}$) (Table 3).

The effect of pH lowering on S^{339}Y-hP2X7R-dependent currents, which represent the P2X7R activation via the high-affinity activation site was also investigated on membrane patch level. ATP application induced noisy inward currents without clear appearance of single-channel currents. This is possibly due to not resolved fast current signals and in accordance with patch currents of truncated hP2X7R receptors which also only display the effect of the high-affinity activation site [27]. Even less strong filtering (5 kHz) did not disclose single-channel current events (Fig. 10A–C). At micromolar [ATP], only strong acidification to pH 5.4 reduced these currents significantly (Fig. 10D). In the patch experiments, high H^+ concentrations were necessary to reduce the effects of ATP probably since the experiments required a free Ca^{2+} concentration of 0.5 mmol/l Ca^{2+} (and therefore also a higher ATP concentration as in the microelectrode experiments using divalent-free extracellular solutions) for patch stabilization. Therefore, the mixture of ATP^{4-} and Ca^{2+} buffered the ATP^{4-} concentration against H^+ binding. These results could simply be explained assuming that the activation of hP2X7R via the high-affinity binding site is only affected by ATP^{4-} binding to protons. The

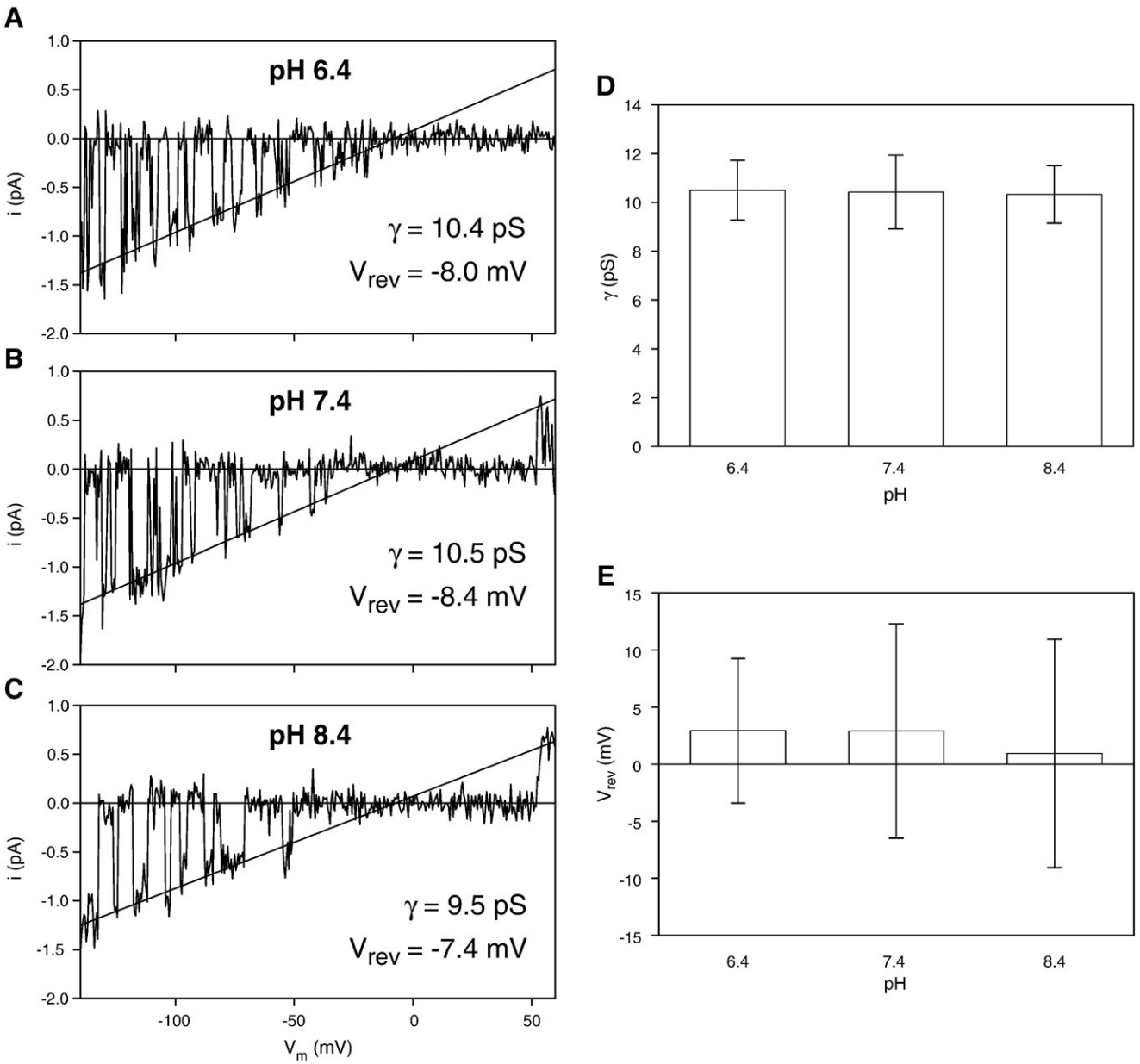

Fig. 6. The effect of the extracellular pH on the single-channel characteristics of the hP2X7R. The figure shows representative single-channel recordings of hP2X7R-mediated currents from outside-out patches that were exposed to different extracellular pH values as indicated. Leak currents and non-specific ATP-induced currents were subtracted [25]. Horizontal lines represent the zero current when the hP2X7R channel in the patch is in the closed state. The currents were recorded during voltage ramp pulses ranging from −140 to +60 mV within 1 s during the activation of the hP2X7R by 1.7 mM (A) or 0.17 mM total ATP (B and C). The straight lines represent linear fits of the open channel current against voltage. The statistical values derived from the fit for slope conductance γ and V_{rev} are shown in D and E, respectively. The data in A–C were obtained from the same patch. The mean values that are shown in D and E were obtained from five patches.

additional allosteric effect of H^+ ions on the other hand is only relevant to hP2X7R activation via the low-affinity activation site.

4. Discussion

Extracellular protons exert different effects on P2X receptor subtypes. While the activation of the P2X1, P2X3, P2X4 and P2X5 receptors was found to be inhibited by lowering the pH of the media [35,36], P2X2 receptors were reported to be potentiated by low pH [37–39]. Using point mutants, the pH effects have been ascribed to the protonation of distinct extracellular histidine residues that are not conserved among the P2XR subtypes [40–42]. In addition, N-linked glycosylation seems to play a role, at least in P2X3 receptors [43].

In rat P2X7R, acidification inhibited the agonist-induced currents [44,45]. A significant part of the inhibiting effect of protons was found to depend on ^{130}His, which was proposed to act as a proton sensor [45]. However, ^{130}His is not conserved in the hP2X7 polypeptide. In a more recent study on the rat P2X7R, alanine replacement of ^{85}His or ^{219}His by alanines was found to increase the proton sensitivity of the resultant mutants severalfold [46]. In addition, simultaneous charge-neutralizing mutations of ^{110}Lys and ^{197}Asp (but not charge-conserving mutations) greatly attenuated the inhibition of the rP2X7R by protons [46]. The P2X7R-dependent uptake of fluorescent dyes (which is generally believed to reflect the induction of pores that are permeable to large organic compounds) was inhibited under both acidic and alkaline conditions [44,47,48].

Here, our detailed analysis of the hP2X7R revealed a rather complex modulation by protons with distinct effects at the previously characterized high- and low-affinity agonist activation sites [26,27]. To specifically assign the effects to either one of the two activation

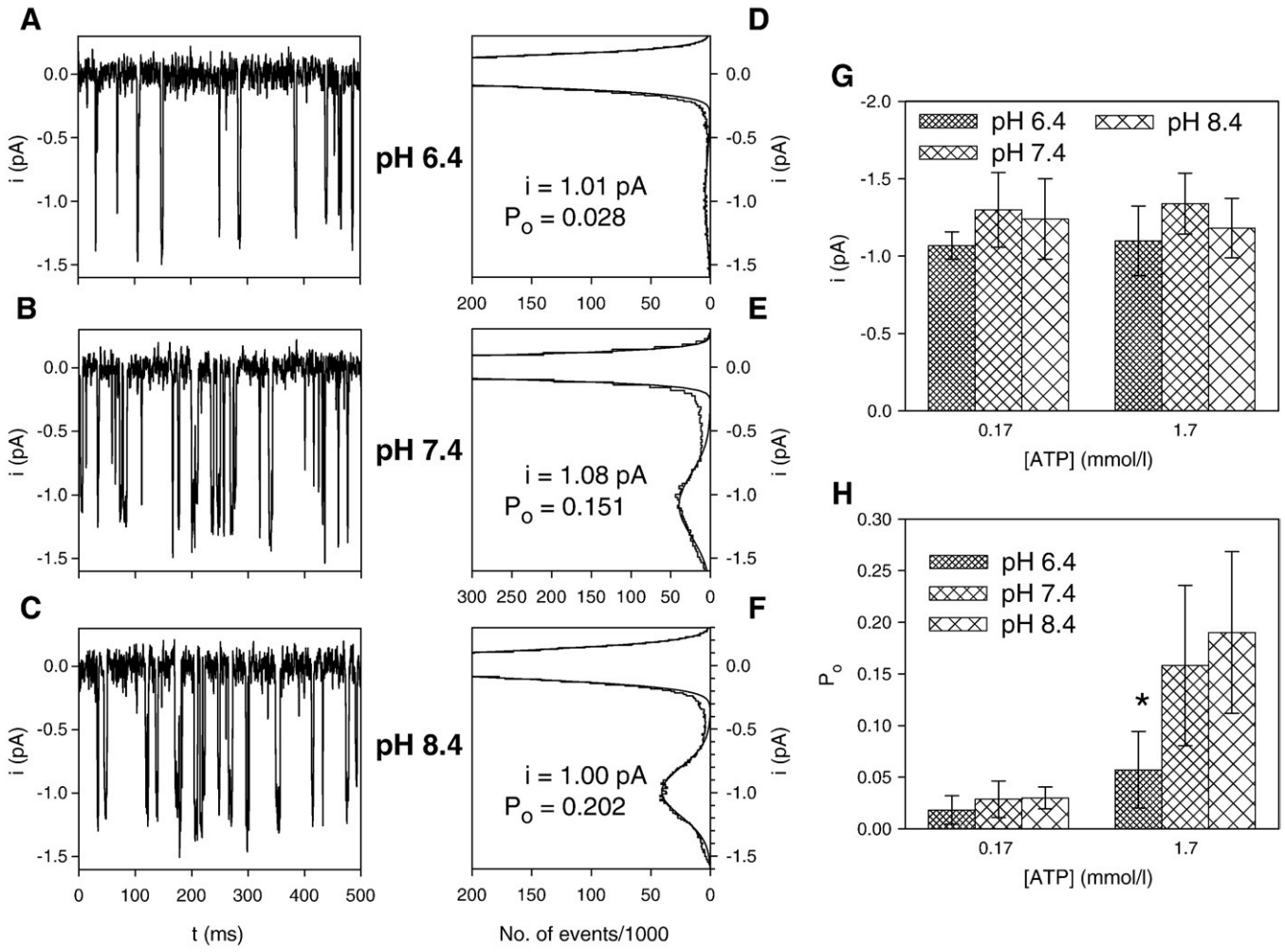

Fig. 7. The effect of the extracellular pH on the hP2X7R single-channel current and the open probability. A–C, Examples of currents recorded from an outside-out membrane patch during the application of 1.7 mM ATP at the indicated extracellular pH. The zero current represents the patch current when the channels are closed. D–F, The amplitude histograms of the corresponding currents that are shown in the adjacent left panels in A–C were fitted by the sum of two Gaussian distributions (smooth solid line) to calculate the mean open channel probability P_o and the single-channel current amplitude i. G, H, The dependences of the single-channel current amplitude and the open probability on the extracellular ATP concentration and the pH were calculated as shown in D–F. The holding potential (V_h) was −120 mV. The mean values that are shown in G and F were obtained from 4 to 23 patches. A statistically significant pH effect is marked by an asterisk.

sites, we exploited several approaches: (i) low and high agonist concentrations were used to activate only the high-affinity site or to activate both activation sites, respectively; (ii) the $S^{339}Y$-hP2X7R mutant (which is activated solely through the high-affinity activation site) allowed current recordings to be made without any contamination by activation through the low-affinity activation site; (iii) the use of high concentrations of BzATP enabled us to predominantly activate the hP2X7R via the low-affinity activation site; and (iv) any contamination by secondarily activated currents could be eliminated by recording single-channel activity from outside-out patches, which completely depend on the activation of the low-affinity activation site of the hP2X7R [27].

4.1. pH-dependent changes in the concentration of ATP^{4-}

The rightward shift of the concentration–response for total ATP for P2X7Rs that is induced by divalent cations is generally considered as evidence that free ATP^{4-} (rather than $MgATP^{2-}$ (or $CaATP^{-2}$)) is the genuine P2X7R agonist [49]. This view is strongly supported by the finding that the divalent-induced shift of the ATP-concentration–response of the human P2X7R can be quantitatively assigned to the pH-dependent change in the concentration of free ATP^{4-} [26,50]. Another strong argument for ATP^{4-} being the agonist of the P2X7R is the present finding that ATP in divalent-free bathing solutions is capable of activating P2X7R-dependent ion currents. However, it is possible that the complexation of ATP^{4-} by divalent cations might exert additional effects on the P2X7R-mediated currents. These may be, for instance, evoked by the newly formed ATP species: $Ca\text{-}ATP^{2-}$ or $Mg\text{-}ATP^{2-}$ or by the free divalent cations. Indeed, not all of the effects of the divalent cations at the P2X7R could be solely explained by ATP^{4-} binding [44].

Here, part of the modulating pH effect on the ATP-dependent activation of the hP2X7R, i.e., the rightward shift of the ATP concentration–response curve, can be assigned to pH-dependent changes in the concentration of ATP^{4-}. This explanation applies to the pH effect on the high- and low-affinity activation sites, analogously to the effects of Mg^{2+} on hP2X7R-dependent currents described previously [26]. Consistent with this view, an alkalinization of the bathing solution from pH 7.4 to 8.4 did not significantly alter the apparent potency of the ATP, as the protonation of ATP^{4-} is only minimally affected by pH changes in this range. According to Eq. (1), decreasing the pH from 7.4 to 6.4 would shift the $\log([ATP^{4-}])$ by −0.29. This matches nearly perfectly the observed shifts in the pK_D values under these conditions (see Table 1). However, even when the concentration–response curves were based on ATP^{4-}, they did not completely overlap at the pH values of 6.4, 7.4 and 8.4 (Fig. 3). This

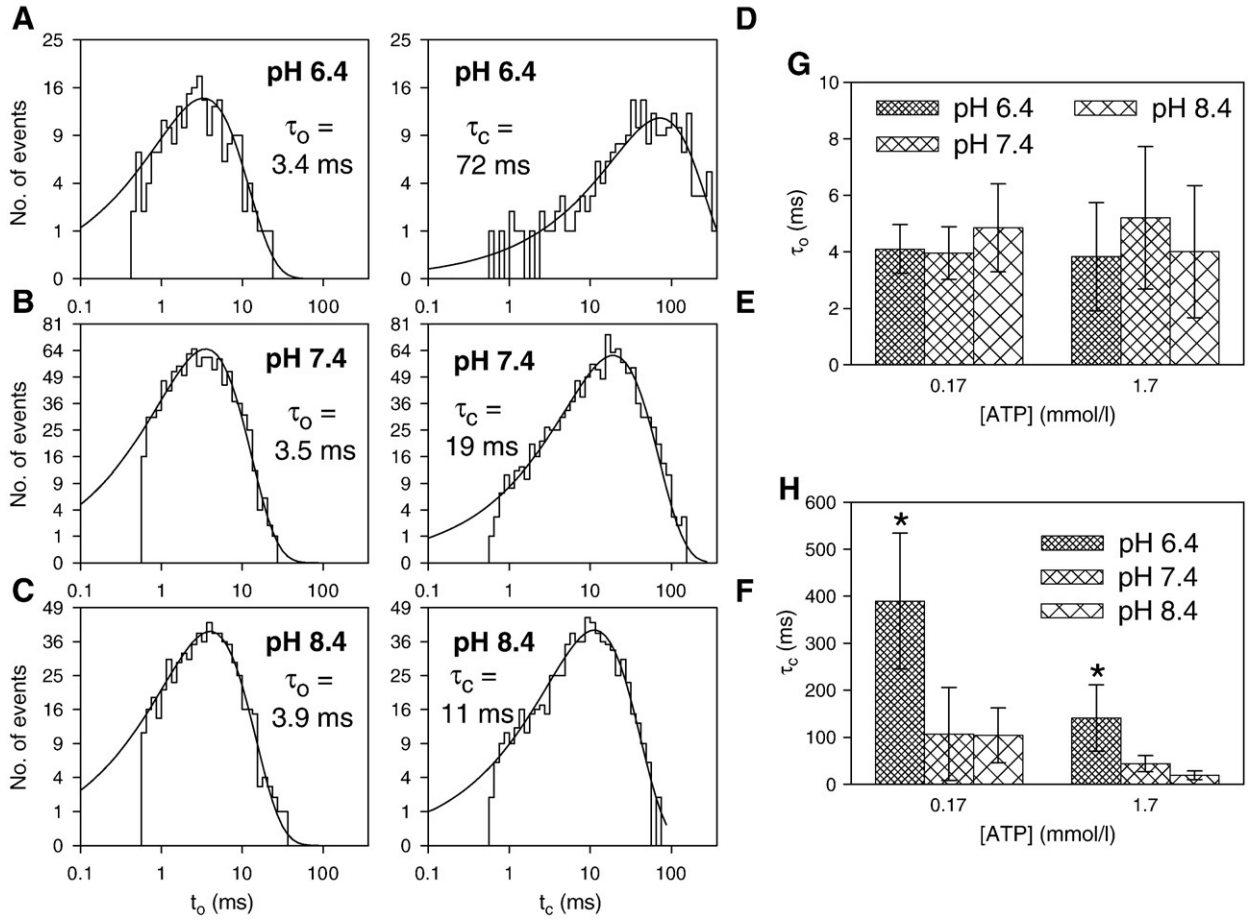

Fig. 8. The effect of the extracellular pH on the kinetics of the hP2X7R single-channel current. Representative open time (A–C) and closed time (D–F) histograms of one outside-out patch in bath solutions containing 1.7 mM ATP with the pH as indicated. G and H, The dependence of the single-channel mean open and closed times, respectively, on the extracellular ATP concentration and pH was calculated as shown in A–F. The holding potential (V_h) was −120 mV. The mean values that are shown in G and F were obtained from 4 to 14 patches. The significant influence of pH is marked by asterisks.

may signify that the proton-binding constants deviate slightly from the published values under our experimental conditions [31]. Alternatively, protons may slightly hamper the binding of ATP^{4-} to the hP2XR. This would be contrary to the observations with the P2X2R, where protons have been suggested to facilitate the binding of negatively charged ATP^{4-}, $CaATP^{2-}$ or $MgATP^{2-}$ [39].

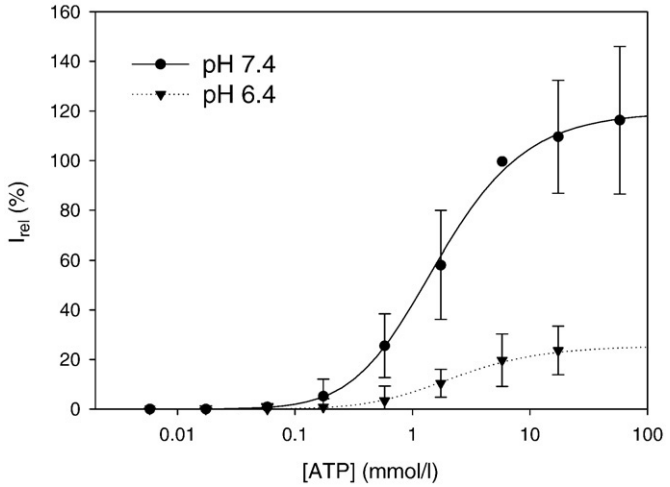

Fig. 9. The influence of acidic pH on the ATP concentration–response behavior at the single hP2X7R channel level. The amplitudes of mean patch currents containing several hP2X7R channels were normalized to the amplitudes using 5.8 mM ATP at pH 7.4 and were approximated by the right term of Eq. (3). The fitted results are given in Table 2. $N = 4–34$ patches.

4.2. Allosteric modulation of the hP2X7R by protons

The most significant effect of acidification is the reduced agonist efficacy at the low-affinity activation site, as reflected by the reduction in the maximal current amplitude that is evoked by high saturating concentrations of ATP or BzATP. Since this effect is not accompanied by a change in the apparent affinity of the agonist binding site, an allosteric modulation effect on the hP2X7R outside the ATP^{4-} binding site is a likely mechanism for this. The single-channel experiments revealed that ion permeation through the hP2XR channel is not affected by external acidification. Therefore, we suggest that protons affect the hP2X7R channel gating subsequent to ATP binding. The location of the protonation site that is responsible is presently unknown. At the rat P2X7R, ^{130}His was found to be critical for the inhibiting effect of extracellular protons [45]. The hP2X7R, however, does not possess a histidine residue at or near position 130 [29].

Table 3
The effect of acidic pH on the activation of single hP2X7R channels.

	$I_{rel,\infty}$ (%)	pK_D
pH 6.4	25 ± 1[a]	3.03 ± 0.03[a]
pH 7.4	120 ± 2	3.16 ± 0.03

The parameters were calculated using Eq. (3) with $I_{rel,\infty,2} = 0$.
[a] Statistically significant differences from values calculated for pH 7.4.

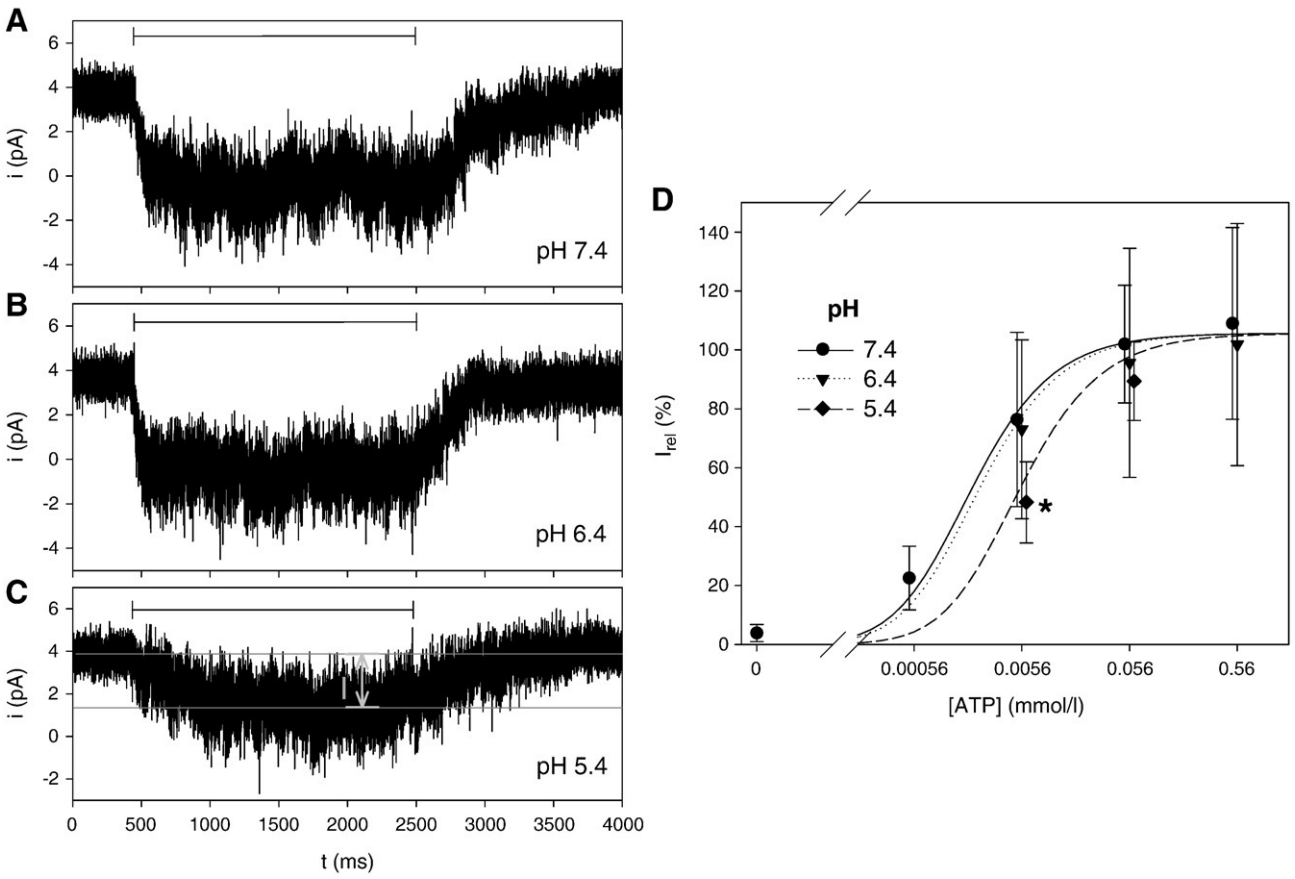

Fig. 10. Effects of pH on patch currents of the S^{339}Y-hP2X7R mutant. A–C, Examples of patch currents induced by 5.6 µmol/l ATP at different pH as indicated. The timing of agonist application (horizontal bars) and the pH of the agonist-containing media are indicated. As demonstrated in C, the mean ATP-induced patch current I was measured as the difference of the mean of the patch current over 300 ms before ATP application and when i reached a saturating inward level. D, Dependence of the mean ATP-induced currents normalized to I (0.056 mM ATP, pH 7.4) on agonist concentration and pH. At the same ATP concentration, only the value marked by an asterisk is significant different from the others. The solid line is the approximation of I_{rel} at pH 7.4 according to the right term of Eq. (3) yielding $pK_{D,1} = -6.1 \pm 0.1$. The other two lines represent the theoretical I_{rel}(ATP) dependence at pH 6.4 and 5.4 as given in the legend assuming simply a reduction of ATP^{4-} by the increasing H^+ concentration. $N = 6$–30 patches.

Although the pK for proton binding is only within a physiologically or pathophysiologically relevant range for histidine residues, proton binding to other amino acids (such as the lysine or aspartic acid of the P2X7R) seems to be functionally important as well [46]. Extensive site-directed mutagenesis may be necessary to identify the allosteric protonation site of the hP2X7R. This may include alanine replacement of the extracellular histidine residues, but other proton-binding amino acids (such as lysine, aspartic acid or glutamic acid) should also be tested.

4.3. Low tissue pH enhances the relative importance of the high-affinity ATP activation site for hP2X7R activation

Cells secrete ATP into the extracellular space in response to hypoxia, inflammation or mechanical stretching, probably by different mechanisms. In addition, necrotic cells release their contents (including intracellular ATP) directly into the interstitial fluid. The bulk concentration of ATP in the extracellular fluids was generally found to be in the nanomolar or low micromolar concentration range [6]. By elaborate methods, the total ATP concentrations were determined to be in the micromolar to (maximally) the 100-µM range near the extracellular membrane surface of ATP-secreting cells [51–54]. However, when the chelation of ATP by extracellular Mg^{2+} and Ca^{2+} and the activity of ectonucleotidases are taken into account, the effective ATP^{4-} concentrations may not exceed the low micromolar range. Accordingly, under physiological or even pathophysiological conditions, the effective ATP concentrations are too low to result in a significant activation of the hP2X7R via the low-affinity activation site. The pH values of inflamed tissue have been reported to be 5.8 to 7.6. Using reliable methods, on average, a drop to a pH value of 6.9 was measured [13]. Under such conditions (under which the release of ATP that may activate the P2X7R is also favored), the importance of the low-affinity activation site for channel activity is further reduced by acidification-induced impaired gating via the low-affinity activation site. Currents induced by micromolar concentrations via the high-affinity ATP binding site, however, are hardly affected by these physiologically and pathophysiologically relevant H^+ concentrations (see Figs. 5C and 10D). It is therefore tempting to conclude from these considerations that the high-affinity activation site is particularly important for hP2X7R channel activity in inflamed tissues.

Acknowledgements

This work was supported by Deutsche Forschungsgemeinschaft Grants Ma1581/12-1 (to F.M.) and Schm536/6-3 (to G. S.) and by the Medical Faculty of the Martin-Luther-University Roux Program Grants 5/09, 10/01 and 13/07 (to F. M.). We thank Mrs. Ursula Braam for the generation of the S^{339}Y-hP2X7R mutant.

References

[1] L.F. Chen, C.F. Brosnan, Regulation of immune response by $P2X_7$ receptor, Crit. Rev. Immunol. 26 (2006) 499–513.
[2] F. Di Virgilio, Liaisons dangereuses: $P2X_7$ and the inflammasome, Trends Pharmacol. Sci. 28 (2007) 465–472.
[3] D. Ferrari, C. Pizzirani, E. Adinolfi, R.M. Lemoli, A. Curti, M. Idzko, E. Panther, F. Di Virgilio, The $P2X_7$ receptor: a key player in IL-1 processing and release, J. Immunol. 176 (2006) 3877–3883.

[4] M.P. Kuehnel, M. Reiss, P.K. Anand, I. Treede, D. Holzer, E. Hoffmann, M. Klapperstueck, T.H. Steinberg, F. Markwardt, G. Griffiths, Sphingosine-1-phosphate receptors stimulate macrophage plasma-membrane actin assembly via ADP release, ATP synthesis and P2X7R activation, J. Cell Sci. 122 (2009) 505–512.
[5] M.P. Kuehnel, V. Rybin, P.K. Anand, E. Anes, G. Griffiths, Lipids regulate P2X7-receptor-dependent actin assembly by phagosomes via ADP translocation and ATP synthesis in the phagosome lumen, J. Cell Sci. 122 (2009) 499–504.
[6] G. Burnstock, Physiology and pathophysiology of purinergic neurotransmission, Physiol. Rev. 87 (2007) 659–797.
[7] S. McGeraughty, M.F. Jarvis, Purinergic control of neuropathic pain, Drug Dev. Res. 67 (2006) 376–388.
[8] C.C. Shieh, M.F. Jarvis, C.H. Lee, R.J. Perner, P2X receptor ligands and pain, Expert Opin. Ther. Patents 16 (2006) 1113–1127.
[9] W.A. Carroll, D. Donnelly-Roberts, M.F. Jarvis, Selective $P2X_7$ receptor antagonists for chronic inflammation and pain, Purinergic Signal. 5 (2009) 63–73.
[10] D.L. Donnelly-Roberts, M.F. Jarvis, Discovery of $P2X_7$ receptor-selective antagonists offers new insights into $P2X_7$ receptor function and indicates a role in chronic pain states, Br. J. Pharmacol. 151 (2007) 571–579.
[11] B.F. King, Novel $P2X_7$ receptor antagonists ease the pain, Br. J. Pharmacol. 151 (2007) 565–567.
[12] R. Romagnoli, P.G. Baraldi, O. Cruz-Lopez, C. Lopez-Cara, D. Preti, P.A. Borea, S. Gessi, The $P2X_7$ receptor as a therapeutic target, Expert Opin. Ther. Targets 12 (2008) 647–661.
[13] A. Punnia-Moorthy, Evaluation of pH changes in inflammation of the subcutaneous air pouch lining in the rat, induced by carrageenan, dextran and *Staphylococcus aureus*, J. Oral Pathol. 16 (1987) 36–44.
[14] F. Marchand, M. Perretti, S.B. McMahon, Role of the immune system in chronic pain, Nat. Rev. Neurosci. 6 (2005) 521–532.
[15] A. Dray, Inflammatory mediators of pain, Br. J. Anaesth. 75 (1995) 125–131.
[16] M. Kress, H.U. Zeilhofer, Capsaicin, protons and heat: new excitement about nociceptors, Trends Pharmacol. Sci. 20 (1999) 112–118.
[17] J.A. Wemmie, M.P. Price, M.J. Welsh, Acid-sensing ion channels: advances, questions and therapeutic opportunities, Trends Neurosci. 29 (2006) 578–586.
[18] E.W. McCleskey, M.S. Gold, Ion channels of nociception, Annu. Rev. Physiol. 61 (1999) 835–856.
[19] R.X. Faria, F.P. DeFarias, L.A. Alves, Are second messengers crucial for opening the pore associated with $P2X_7$ receptor? Am. J. Physiol. 288 (2005) C260–C271.
[20] P. Pelegrin, A. Surprenant, Pannexin-1 mediates large pore formation and interleukin-1 release by the ATP-gated $P2X_7$ receptor, EMBO J. 25 (2006) 5071–5082.
[21] R. Iglesias, S. Locovei, A.P. Roque, A.P. Alberto, G. Dahl, D.C. Spray, E. Scemes, $P2X_7$ receptor–Pannexin1 complex: pharmacology and signaling, Am. J. Physiol. 295 (2008) C752–C760.
[22] J. Schachter, A.P. Motta, A.D. de Souza Zamorano, H.A. Silva-Souza, M.Z. Guimaraes, P.M. Persechini, ATP-induced P2X7-associated uptake of large molecules involves distinct mechanisms for cations and anions in macrophages, J. Cell Sci. 121 (2008) 3261–3270.
[23] R.A. North, Molecular physiology of P2X receptors, Physiol. Rev. 82 (2002) 1013–1067.
[24] M. Klapperstück, C. Büttner, T. Böhm, G. Schmalzing, F. Markwardt, Characteristics of $P2X_7$ receptors from human B lymphocytes expressed in *Xenopus* oocytes, Biochim. Biophys. Acta 1467 (2000) 444–456.
[25] T. Riedel, I. Lozinsky, G. Schmalzing, F. Markwardt, Kinetics of $P2X_7$ receptor-operated single channels currents, Biophys. J. 92 (2007) 2377–2391.
[26] M. Klapperstück, C. Büttner, G. Schmalzing, F. Markwardt, Functional evidence of distinct ATP activation sites at the human $P2X_7$ receptor, J. Physiol. (Lond.) 534 (2001) 25–35.
[27] D. Becker, R. Woltersdorf, W. Boldt, S. Schmitz, U. Braam, G. Schmalzing, F. Markwardt, The $P2X_7$ carboxyl tail is a regulatory module of $P2X_7$ receptor channel activity, J. Biol. Chem. 283 (2008) 25725–25734.
[28] G.B. Drummond, Reporting ethical matters in The Journal of Physiology: standards and advice, J. Physiol. (Lond.) 587 (2009) 713–719.
[29] F. Rassendren, G.N. Buell, C. Virginio, G. Collo, R.A. North, A. Surprenant, The permeabilizing ATP receptor, $P2X_7$ — cloning and expression of a human cDNA, J. Biol. Chem. 272 (1997) 5482–5486.
[30] F. Bretschneider, F. Markwardt, Drug-dependent ion channel gating by application of concentration jumps using U-tube technique, Methods Enzymol. 294 (1999) 180–189.
[31] A.M. Martell, R.M. Smith, Amines, Plenum Press, New York, 1990.
[32] F. Markwardt, G. Isenberg, Gating of maxi K^+ channels studied by Ca^{2+} concentration jumps in excised inside-out multi-channel patches (myocytes from guinea pig urinary bladder), J. Gen. Physiol. 99 (1992) 841–862.
[33] B.U. Failer, A. Aschrafi, G. Schmalzing, H. Zimmermann, Determination of native oligomeric state and substrate specificity of rat NTPDase1 and NTPDase2 after heterologous expression in *Xenopus* oocytes, Eur. J. Biochem. 270 (2003) 1802–1809.
[34] R. Horn, Statistical methods for model discrimination: application to gating kinetics and permeation of the acetylcholine receptor channel, Biophys. J. 51 (1987) 255–263.
[35] R. Stoop, A. Surprenant, R.A. North, Different sensitivities to pH of ATP-induced currents at four cloned P2X receptors, J. Neurophysiol. 78 (1997) 1837–1840.
[36] S.S. Wildman, S.G. Brown, M. Rahman, C.A. Noel, L. Churchill, G. Burnstock, R.J. Unwin, B.F. King, Sensitization by extracellular Ca^{2+} of rat $P2X_5$ receptor and its pharmacological properties compared with rat $P2X_1$, Mol. Pharmacol. 62 (2002) 957–966.
[37] B.F. King, L.E. Ziganshina, J. Pintor, G. Burnstock, Full sensitivity of P_{2X2} purinoceptor to ATP revealed by changing extracellular pH, Br. J. Pharmacol. 117 (1996) 1371–1373.
[38] S.H. Ding, F. Sachs, Single channel properties of $P2X_2$ purinoceptors, J. Gen. Physiol. 113 (1999) 695–719.
[39] A. Skorinkin, A. Nistri, R. Giniatullin, Bimodal action of protons on ATP currents of rat PC12 cells, J. Gen. Physiol. 122 (2003) 33–44.
[40] C.E. Clarke, C.D. Benham, A. Bridges, A.R. George, H.J. Meadows, Mutation of histidine 286 of the human $P2X_4$ purinoceptor removes extracellular pH sensitivity, J. Physiol. (Lond.) 523 (2000) 697–703.
[41] J.D. Clyne, L.D. LaPointe, R.I. Hume, The role of histidine residues in modulation of the rat $P2X_2$ purineceptor by zinc and pH, J. Physiol. (Lond.) 539 (2002) 347–359.
[42] Z. Gerevich, Z.S. Zadori, L. Koles, L. Kopp, D. Milius, K. Wirkner, K. Gyires, P. Illes, Dual effect of acid pH on purinergic $P2X_3$ receptors depends on the histidine-206 residue, J. Biol. Chem. 282 (2007) 33949–33957.
[43] K. Wirkner, D. Stanchev, D. Milius, L. Hartmann, E. Kato, Z.S. Zadori, P.P. Mager, P. Rubini, W. Nörenberg, P. Illes, Regulation of the pH sensitivity of human $P2X_3$ receptors by N-linked glycosylation, J. Neurochem. 107 (2008) 1216–1224.
[44] C. Virginio, D. Church, R.A. North, A. Surprenant, Effects of divalent cations, protons and calmidazolium at the rat $P2X_7$ receptor, Neuropharmacology 36 (1997) 1285–1294.
[45] C. Acuna-Castillo, C. Coddou, P. Bull, J. Brito, J.P. Huidobro-Toro, Differential role of extracellular histidines in copper, zinc, magnesium and proton modulation of the $P2X_7$ purinergic receptor, J. Neurochem. 101 (2007) 17–26.
[46] X. Liu, W. Ma, A. Surprenant, L.H. Jiang, Identification of the amino acid residues in the extracellular domain of rat P2X7 receptor involved in functional inhibition by acidic pH, Br. J. Pharmacol. 156 (2009) 135–142.
[47] T.H. Steinberg, A.S. Newman, J.A. Swanson, S.C. Silverstein, ATP^{4-} permeabilizes the plasma membrane of mouse macrophages to fluorescent dyes, J. Biol. Chem. 262 (1987) 8884–8888.
[48] A.D. Michel, I.P. Chessell, P.P.A. Humphrey, Ionic effects on human recombinant $P2X_7$ receptor function, Naunyn-Schmiedeberg's Arch. Pharmacol. 359 (1999) 102–109.
[49] F. Di Virgilio, P. Chiozzi, S. Falzoni, D. Ferrari, J.M. Sanz, V. Venketaraman, O.R. Baricordi, Cytolytic P2X purinoceptors, Cell Death Differ. 5 (1998) 191–199.
[50] F. Markwardt, M. Löhn, T. Böhm, M. Klapperstück, Purinoceptor-operated cationic channels in human B lymphocytes, J. Physiol. (Lond.) 498 (1997) 143–151.
[51] E.A. Newman, Propagation of intercellular calcium waves in retinal astrocytes and Müller cells, J. Neurosci. 21 (2001) 2215–2223.
[52] P. Pellegatti, S. Falzoni, P. Pinton, R. Rizzuto, F. Di Virgilio, A novel recombinant plasma membrane-targeted luciferase reveals a new pathway for ATP secretion, Mol. Biol. Cell 16 (2005) 3659–3665.
[53] A.V. Gourine, N. Dale, E. Llaudet, D. Poputnikov, K.M. Spyer, V.N. Gourine, Release of ATP in the central nervous system during systemic inflammation: real-time measurement in the hypothalamus of conscious rabbits, J. Physiol. (Lond.) 305–16 (Pt 1) (2007) 305–316.
[54] R. Beigi, E. Kobatake, M. Aizawa, G.R. Dubyak, Detection of local ATP release from activated platelets using cell surface-attached firefly luciferase, Am. J. Physiol. 276 (1999) C267–C278.